Catalytic doping of phosphorus and boron atoms onto hydrogenated amorphous silicon films

Junichi Seto[1,2], Keisuke Ohdaira[1,2*], and Hideki Matsumura[1,2]

[1]*Japan Advanced Institute of Science and Technology, 1-1 Asahidai, Nomi, Ishikawa 923-1292, Japan*

[2]*CREST, Japan Science and Technology Agency (JST), Kawaguchi, Saitama 332-0012, Japan*

E-mail: ohdaira@jaist.ac.jp

We investigate the low temperature doping of phosphorus (P) and boron (B) atoms onto hydrogenated amorphous silicon (a-Si:H) films by catalytic doping (Cat-doping). The conductivity of a-Si:H films increases as catalyzer temperature (T_{cat}) increases, and the increase in the conductivity is accompanied by significant reduction in the activation energy obtained from the Arrhenius plot of the conductivity. Secondary ion mass spectrometry (SIMS) measurement reveals that Cat-doped P and B atoms exist within ~10-15 nm from the surface of a-Si:H films, indicating that the shallow doping of P and B atoms is realized onto a-Si:H films like the case of Cat-doping onto crystalline Si (c-Si) wafers. We also confirm no additional film deposition during Cat-doping. These results suggest that decomposed species are effectively doped onto a-Si:H films similar to the case of Cat-doping onto c-Si.

1. Introduction

In recent years, solar power generation has been getting a lot of attention as one of major renewable energy resources. Of many types of solar cells, crystalline silicon (c-Si) has been used most widely as a photovoltaic material. Silicon heterojunction (SHJ) solar cells have attracted much attention because of their high energy conversion efficiency.[1–15] A SHJ solar cell consists of intrinsic and doped hydrogenated amorphous silicon (a-Si:H) films with each thickness of ~10 nm and a crystalline Si (c-Si) wafer as well as transparent conductive oxide (TCO) layers and metal electrodes. Taguchi *et al*. have recently reported a large-area area conventional SHJ solar cell with a high conversion efficiency of 24.7%.[14] Furthermore, Masuko *et al*. have reported a large-area heterojunction back-contact (HBC) solar cell with the highest efficiency of 25.6%.[15] Such HBC cells, however, particularly requires complicated fabrication process including photolithography, compared with conventional c-Si solar cells. This results in higher fabrication cost, which cannot be acceptable for their mass-production. A simpler process to locally form p- and n-type a-Si:H layers is thus required. In addition, the fabrication process must be performed at low temperatures of below 200 °C, since the a-Si:H layers generally have low thermal tolerance.

We have so far demonstrated that shallow boron (B)- or phosphorus (P)-doped layers can be formed by exposing c-Si surfaces to P or B-related radicals generated by the catalytic cracking of phosphine (PH_3) or diborane (B_2H_6) gas molecules on a heated tungsten (W) catalyzer.[16–23] This method, catalytic doping (Cat-doping), can be performed at substrate temperatures of less than 200 °C, and the doped layers formed by Cat-doping are as shallow as <5 nm.[24] Thus, if Cat-doping can be effectively applied also for a-Si:H films, the fabrication process of HBC cells will be significantly simplified. This is because patterned p- and n-type a-Si:H layers can be easily formed by the deposition of intrinsic a-Si:H (i-a-Si:H) films and successive Cat-doping of P and B atoms onto the a-Si:H layer through patterned hard masks.

In this paper, we investigate B and P Cat-doping onto a-Si:H films. a-Si:H films receiving B and P Cat-doping have significantly higher conductivity than original a-Si:H films. The activation energy (E_a) of the conductivity of Cat-doped a-Si:H films is also definitely smaller than that of a-Si:H films. These indicate that Cat-doping is effective also

for a-Si:H films as well as for c-Si wafers. Secondary ion mass spectrometry (SIMS) measurement clarifies the thickness of P and B Ca-doped layers to be about 10-15 nm.

2. Experimental methods

19.8×19.8×0.4 mm^3-sized Corning Eagle glass was used as substrates. i-a-Si:H films with a thickness of ~20 nm were deposited on the glass substrates by catalytic chemical vapor deposition (Cat-CVD) under the conditions summarized in Table I. The thickness of i-a-Si:H films was measured by spectroscopic ellipsometry. P or B Cat-doping was then performed onto the i-a-Si:H films, whose conditions are also summarized in Table I. Substrate temperature (T_{sub}) and catalyzer temperature (T_{cat}) during Cat-doping were systematically changed. Since the decomposition of B_2H_6 molecules is promoted in the presence of H_2 gas flow,[25] B Cat-doping was also performed with H_2 gas flow under the condition summarized in Table I. Under the H_2 flow during Cat-doping, H radicals generated by catalytic cracking can etch i-a-Si:H films. To protect a-Si:H films from etching by H radicals, we formed ultra-thin oxide layers on the surfaces of an i-a-Si:H films by dipping in 30 wt% H_2O_2 for 10 min only before B Cat-doping with H_2 flow.[26]

Al coplanar electrodes were evaporated through a hard mask on the P or B Cat-doped a-Si:H films to evaluate their conductivity from I-V curves. The conductivities were calculated simply by using an i-a-Si:H film thickness of 20 nm. The ultra-thin oxide layers formed by H_2O_2 dipping were removed by HF dipping prior to the evaporation of Al electrodes. I-V characteristics were measured on a semiconductor parameter analyzer. The E_a of the conductivity of Cat-doped a-Si:H films was obtained by changing the temperature of the samples from 50 to 150 °C at intervals of 20 °C during I-V measurement and by using Arrhenius equation.

In order to check the deposition of a-Si:H films during Cat-doping due to the generation of Si-related radicals from a-Si:H existing on chamber walls, we also performed Cat-doping onto bare glass substrates and measured their optical transmittance. The thicknesses of P and B Cat-doped layers in a-Si:H were characterized by SIMS measurement. P Cat-doping was performed onto 70 nm-thick i-a-Si:H films deposited on p-type c-Si wafers, while B Cat-doping was conducted onto 70 nm-thick a-Si:H films formed on n-type c-Si wafers under the condition summarized in Table II. The 70 nm-thick a-Si:H films were prepared

under the conditions shown in Table II. SIMS profiles were measured from the back sides of the samples after thinning c-Si wafer in order to avoid the effect of knock-on and resulting unexpected broadening of B and P profiles.

3. Results and discussion

We have first confirmed the absence of unintentional a-Si deposition during Cat-doping process using transparent glass substrates. If doped a-Si:H is deposited during Cat-doping, the optical transmittance of glass substrates in short wavelength region must decrease due to optical absorption in a-Si:H. The transmittance of glass substrates after Cat-doping, however, does not decrease at all. This result indicates that n- and p-a-Si:H films are not deposited during Cat-doping, and increase in the conductivity of a-Si films by Cat-doping shown below is caused by the Cat-doping of P or B atoms onto a-Si films.

Figure 1 shows the conductivity of a-Si:H films after P Cat-doping at various T_{sub} as a function of T_{cat}. The conductivity of an i-a-Si:H film without receiving Cat-doping was 6.8×10^{-11} S/cm, which is a typical conductivity of i-a-Si:H. The a-Si:H films Cat-doped at T_{cat} of less than 1100 °C have conductivities similar to that of i-a-Si:H. On the other hand, the conductivities of Cat-doped a-Si:H films increase at T_{cat} of 1100 °C or more. PH_3 molecules are decomposed to P and H radicals by catalytic cracking on a W catalyzer heated at more than 1000 °C, and the amount of such radicals increases exponentially as T_{cat} increases.[27–29] The catalytic cracking of PH_3 molecules is promoted by an increase in T_{cat}, which probably leads to more effective doping of P atoms. The conductivities of a-Si:H films Cat-doped at every T_{sub} also show similar dependence on T_{cat}. This fact indicate that P Cat-doping onto a-Si:H films is at least partially dominated by the reactivity of P-related radicals.

Figure 2(a) shows the conductivity of a-Si:H films after B Cat-doping at T_{sub} from 50 to 200 °C as a function of T_{cat}. These conductivities show a tendency similar to the case of P Cat-doping, and increases almost monotonically with T_{cat}. The decomposition of B_2H_6 molecules is probably enhanced by increase in T_{cat}, which may be the reason for the increased conductivity. Figure 2(b) shows the conductivity of a-Si:H films after B Cat-doping at T_{sub} from 250 to 350 °C as a function of T_{cat}. Unlike the case of lower T_{sub}, the conductivity is almost independent of T_{cat}, and is relatively high even under no heating

of a catalyzing wire compared to that of a-Si:H films without B Cat-doping. These facts mean that active B-related radicals are related to B Cat-doping at low T_{sub}, while thermal process on the surfaces of a-Si:H films is dominant at higher T_{sub}. This can be confirmed more clearly in Fig. 2(c), in which the conductivity of a-Si:H films after exposure to B_2H_6 flow without heating a catalyzing wire is plotted as a function of T_{sub}. The conductivity of a-Si:H films starts to increase at a T_{sub} of ~250 °C. This result is quantitatively reasonable since the thermal decomposition of B_2H_6 molecules can occur effectively at 250 °C.[30-31)]

Figures 3(a) and (b) shows the E_a of the conductivity of P and B Cat-doped a-Si:H films as a function of T_{cat}, respectively, in which Cat-doping was performed at T_{sub} of 150 and 350 °C. The E_a of the conductivity of i-a-Si:H was 0.85 eV, which corresponds to the half of the band gap of i-a-Si:H used in this study. P and B Cat-doped a-Si:H films have much smaller E_a, as shown in Figs. 3(a) and (b). This is also a clear experimental evidence of the formation of doped layers by Cat-doping. In the case of P Cat-doping, E_a decreases monotonically with increase in T_{cat}. The E_a of the conductivity of a-Si:H films P Cat-doped at a T_{sub} of 350 °C have much lower E_a than that of a-Si:H films at a T_{sub} of 150 °C, particularly at high T_{cat}. This fact might indicate more effective doping of P atoms at higher T_{cat} and higher activation rate of P atoms at higher T_{sub}. The E_a of the conductivity of a-Si:H films B Cat-doped at a T_{sub} of 150 °C decreases with increase in T_{cat}, similar to the case of P Cat-doping. On the contrary, The E_a of the conductivity of a-Si:H films B Cat-doped at a T_{sub} of 350 °C is almost independent of T_{cat} and is smaller than the E_a of the conductivity of an intrinsic a-Si:H film even at low T_{cat}. These can also be explained by the dominant contribution of B-related radicals generated by the catalytic decomposition of B_2H_6 molecules and the emergence of the thermal decomposition of B_2H_6 molecules at a T_{sub} of >250 °C, as mentioned above.

In order to enhance the effect of B doping, we have attempted to add H_2 gas flow during Cat-doping. Figure 4 shows the conductivities of B Cat-doped a-Si:H films as a function of H_2 flow rate. The conductivity of a-Si:H films increase with H_2 flow rate up to 40 sccm. The increase in the conductivity of a-Si:H films with the addition of H_2 may be due to more enhanced decomposition of B_2H_6 molecules through reaction with H radicals in vapor phase.[25)]

Figure 5 shows the SIMS profiles of Cat-doped P and B atoms in a-Si:H films. P and B

atoms are not distributed uniformly but exist locally in the vicinity of the surfaces of a-Si:H films. The depths of P- and B-doped layers are within 10-15 nm. The slightly broader profile of B atoms shown in the SIMS profile might be related to the addition of H_2 during Cat-doping and resulting etching of an a-Si surface by atomic hydrogen. Note that the conductivities of P or B Cat-doped a-Si:H films shown above were estimated by using the a-Si:H thickness of 20 nm. Based on the dopant profiles revealed by SIMS measurement, the actual conductivities of Cat-doped a-Si:H layers must be much higher, although the precise determination of their conductivity is difficult since P and B atoms are distributed ununiformly.

The feature of Cat-doping within 10-15 nm from the surface of a-Si:H films will be beneficial for the fabrication of SHJ solar cells. The fabrication process of SHJ solar cells can be simplified as follows. i-a-Si:H films with a thickness of about 20 nm are first deposited on both sides of a c-Si wafer. P and B Cat-doping are then performed on the i-a-Si:H films. The doping depth is automatically limited to be ~10 nm, intrinsic a-Si:H region will remain at the a-Si:H/c-Si interfaces, which will effectively act as passivation layers. The fabrication of HBC solar cells may also be possible through the same process flow. The partial formation of p- and n-type regions may be realized by Cat-doping through hard masks.

4. Conclusions

We have confirmed the effectiveness of P and B Cat-doping onto a-Si:H films. Cat-doping onto a-Si:H films leads to increase in their conductivities accompanied by decreases in E_a. An increase in the conductivity of a-Si:H films is enhanced at higher T_{cat}, which is because of more efficient decomposition of dopant gas molecules and resulting formation of more radicals. The addition of H_2 during B Cat-doping results in the enhancement of doping effect, probably because of more effective decomposition of B_2H_6 molecules through gas phase reaction. Cat-doped P and B atoms exist within 10-15 nm from the surface of a-Si:H films. The Cat-doping of P and B atoms onto a-Si:H films will be utilized for the fabrication of SHJ and HBC solar cells.

Acknowledgments

This work was supported by Core Research for Evolutional Science and Technology (CREST) Japan Science and Technology Agency (JST) program. The authors would like to thank Prof. H. Umemoto of Shizuoka University for his helpful advice. The authors would also like to thank Dr. Koichi Koyama of JAIST for fruitful discussion.

References

1) S. De Wolf, A. Descoeudres, Z. C. Holman, and C. Ballif, Green **2**, 7 (2012).
2) J. Nakamura, N. Asano, T. Hieda, C. Okamoto, H. Katayama, and K. Nakamura, IEEE J. Photovolt. **4** 1491 (2014).
3) J.L. Hernandez, D. Adachi, D. Schroos, N. Valckx, N. Menou, T. Uto, M. Hino, M. Kanematsu, H. Kawasaki, R. Mishima, K. Nakano, H. Uzu, T. Terashita, K. Yoshikawa, T. Kuchiyama, M. Hiraishi, N. Nakanishi, M. Yoshimi, and K. Yamamoto, Proc. 28th European Photovoltaic Solar Energy Conf., 2013, p. 741.
4) A. Descoeudres, Z. C. Holman, L. Barraud, S. Morel, S. De Wolf, and C. Ballif, IEEE J. Photovoltaics **3**, 83 (2013).
5) F. Jay, D. Muñoz, T. Desrues, E. Pihan, V. A. de Oliveira, and N. Enjalbert, Sol. Energy Mater. Sol. Cells **130**, 690 (2014).
6) K. Nakada, J. Irikawa, S. Miyajima, and M. Konagai, Jpn. J. Appl. Phys. **54**, 052303 (2015).
7) H. Fujiwara, H. Sai, and M. Kondo, Jpn. J. Appl. Phys. **48**, 064506 (2009).
8) M. Taguchi, E. Maruyama, and M. Tanaka, Jpn. J. Appl. Phys. **47**, 814 (2008).
9) J. Ziegler, A. Montesdeoca-Santana, D. Platt, S. Hohage, R. GuerreroLemus, and D. Borchert, Jpn. J. Appl. Phys. **51**, 10NA03 (2012).
10) D. Thibaut, V. De Sylvain, S. Florent, D. Djicknoum, M. Delfina, G.-F. Marie, K. Jean-Paul, and R. Pierre-Jean, Energy Procedia **8**, 294 (2011).
11) A. Tomasi, B. Paviet-Salomon, D. Lachenal, S. M. de Nicolas, A. Descoeudres, J. Geissbuhler, S. De Wolf, and C. Ballif, IEEE J. Photovoltaics **4**, 1046 (2014).
12) Z. Shu, U. Das, J. Allen, R. Birkmire, and S. Hegedus, Prog. Photovoltaics **23**, 78 (2015).
13) N. Mingirulli, J. Haschke, R. Gogolin, R. Ferré, T. F. Schulze, J. Düsterhöft, N.-P. Harder, L. Korte, R. Brendel, and B. Rech, Phys. Status Solidi: Rapid Res. Lett. **5**, 159 (2011).
14) M. Taguchi, A. Yano, S. Tohoda, K. Matsuyama, Y. Nakamura, T. Nishiwaki, K. Fujita, and E. Maruyama, IEEE J. Photovoltaics **4**, 96 (2014).
15) K. Masuko, M. Shigematsu, T. Hashiguchi, D. Fujishima, M. Kai, N. Yoshimura,T. Yamaguchi, Y. Ichihashi, T. Mishima, N. Matsubara, T. Yamanishi, T. Takahama, M. Taguchi, E. Maruyama, and S. Okamoto, IEEE J. Photovoltaics **4**, 1433 (2014).
16) S. Tsuzaki, K. Ohdaira, T. Oikawa, K. Koyama, and H. Matsumura, Jpn. J. Appl. Phys. **54**,

072301 (2015).
17) T. Ohta, K. Koyama, K. Ohdaira, and H. Matsumura, Thin Solid Films **575**, 92 (2015)
18) Trinh Cham Thi, K. Koyama, K. Ohdaira, and H. Matsumura, J. Appl. Phys. **116**, 044510 (2014).
19) T. Hayakawa, T. Ohta, Y. Nakashima, K. Koyama, K. Ohdaira, and H. Matsumura, Jpn. J. Appl. Phys **51**, 101301 (2012).
20) T. Hayakawa, Y. Nakashima, K. Koyama, K. Ohdaira, and H. Matsumura, Jpn. J. Appl. Phys. **51**, 061301 (2012).
21) T. Hayakawa, Y. Nakashima, M. Miyamoto, K. Koyama, K. Ohdaira, and H. Matsumura, Jpn. J. Appl. Phys. **50**, 121301 (2011).
22) T. Hayakawa, M. Miyamoto, K. Koyama, K. Ohdaira, and H. Matsumura, Thin Solid Films **519**, 4466 (2011).
23) H. Matsumura, M. Miyamoto, K. Koyama, and K. Ohdaira, Sol. Energy Mater. Sol. Cells **95**, 797 (2011).
24) H. Matsumura, T. Hayakawa, T. Ohta, Y. Nakashima, M. Miyamoto, Trinh Cham Thi, K. Koyama, and K. Ohdaira, J. Appl. Phys. **116**, 114502 (2014).
25) H. Umemoto, T. Kanemitsu and Akihito Tanaka, J. Phys. Chem. A **118**, 5156 (2014).
26) T. Oikawa, K. Ohdaira, K. Higashimine and H. Matsumura, Current Appl. Phys. **15**, 1168 (2015).
27) H. Umemoto, Y. Nishihara, T. Ishikawa, and S. Yamamoto, Jpn. J. Appl. Phys. **51**, 086501 (2012).
28) H. Umemoto, Thin Solid Films **575,** 9 (2015).
29) H. Umemoto, T. Kanemitsu, and Y. Kuroda, Jpn. J. Appl. Phys. **53**, 05FM02 (2014).
30) M. Söderlund, P. Mäki-Arvela, K. Eränen, T. Salmi, R. Rahkola, and D. Yu. Murzin, Catal. Lett. **105**, 191 (2005).
31) H. Habuka, S. Akiyama, T. Otsuka, and W. F. Qu, J. Cryst. Growth **209**, 807 (2000).

Figure Captions

Fig. 1. (Color online) Conductivity of P Cat-doped a-Si:H films at various T_{sub} as a function of T_{cat}.

Fig. 2. (Color online) Conductivity of B Cat-doped a-Si:H films as a function of T_{cat} at T_{sub} of (a) ≤200 °C and (b) ≥250 °C. (c) Conductivity of the a-Si:H films after exposure to B_2H_6 flow without heating a catalyzing wire as a function of T_{sub}.

Fig. 3. (Color online) E_a of the conductivity of (a) P and (b) B Cat-doped a-Si:H films as a function of T_{cat} at T_{sub} of 150 and 350 °C.

Fig. 4. (Color online) Conductivities of B doped a-Si:H films as a function of H_2 flow rate.

Fig. 5. (Color online) SIMS profiles of Cat-doped (a) P and (b) B atoms in a-Si:H films. Dash lines indicate detection limits in the SIMS measurement.

Table I. Conditions of i-a-Si:H film deposition and P or B Cat-doping.

	T_{sub} (°C)	T_{cat} (°C)	Duration (s)	Pressure (Pa)	Gas	Flow rate (sccm)
i-a-Si:H	160	1800	90	1	SiH_4	10
P doping	50–350	R.T.–1700	300	2	2.25% PH_3 (He-diluted)	20
B doping	50–350	R.T.–1800	300	2	2.25% B_2H_6 (He-diluted)	20
B doping (with H_2 flow)	350	1800	300	3.9	2.25% B_2H_6 (He-diluted)	20
					H_2	0–60

Table II. Conditions of i-a-Si:H film deposition and P or B Cat-doping for SIMS measurement.

	T_{sub} (°C)	T_{cat} (°C)	Duration (s)	Pressure (Pa)	Gas	Flow rate (sccm)
i-a-Si:H	160	1800	400	1	SiH_4	10
P doping	300	1500	300	2	2.25% PH_3 (He-diluted)	20
B doping	350	1800	300	3.9	2.25% B_2H_6 (He-diluted)	20
					H_2	40

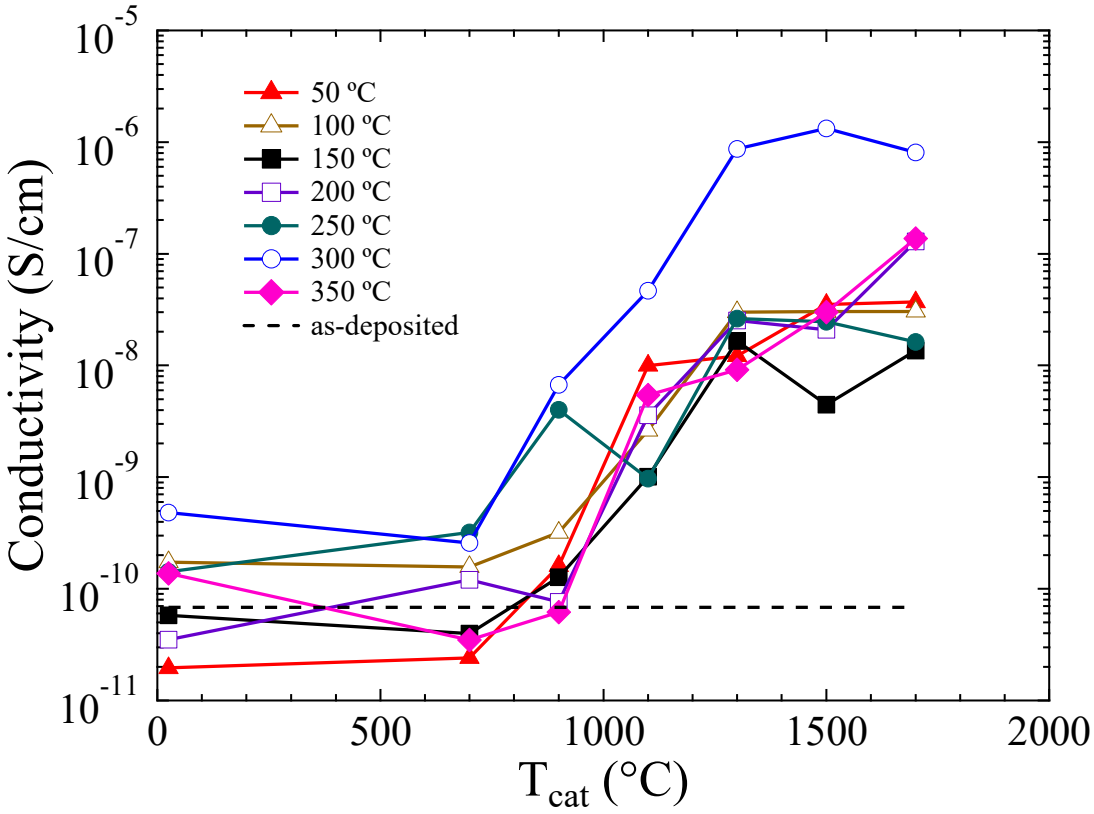

Fig. 1. (Color online)

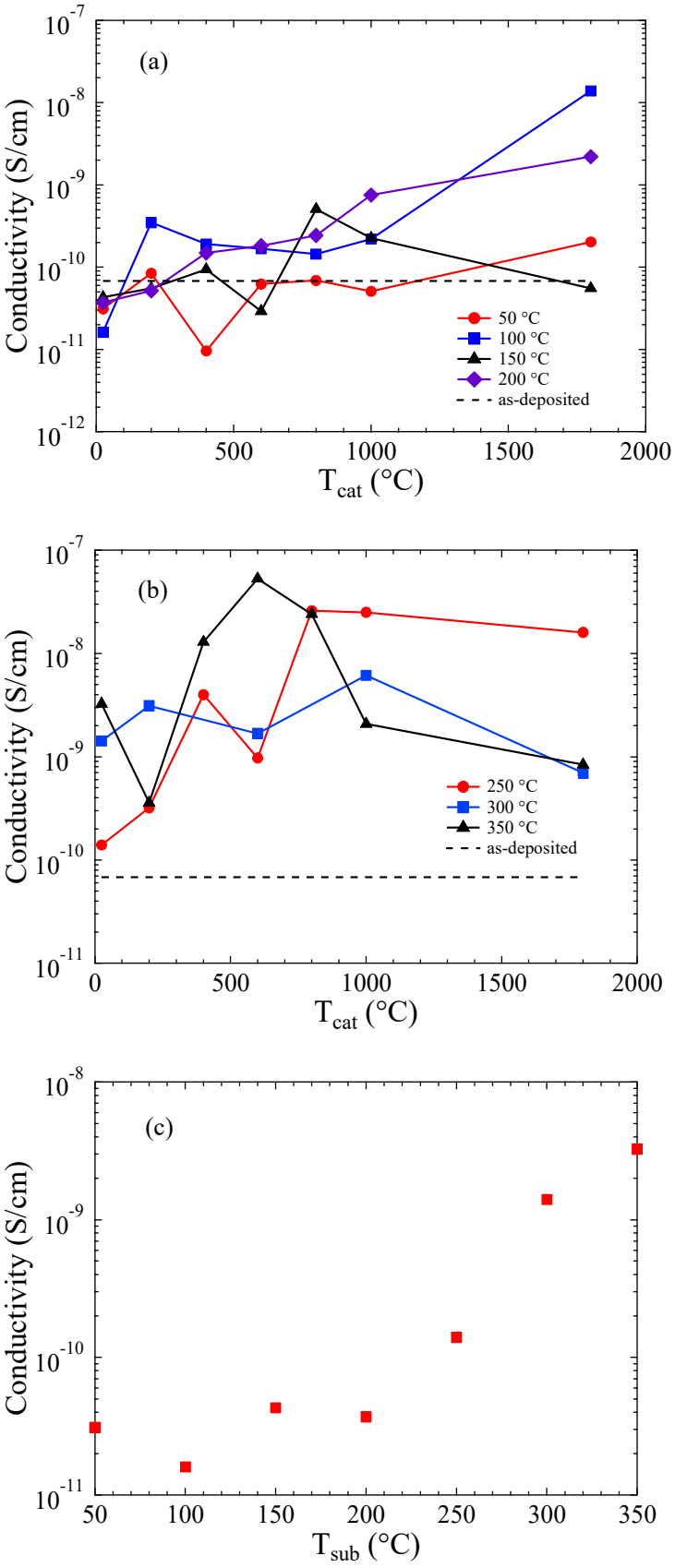

Fig. 2. (Color online)

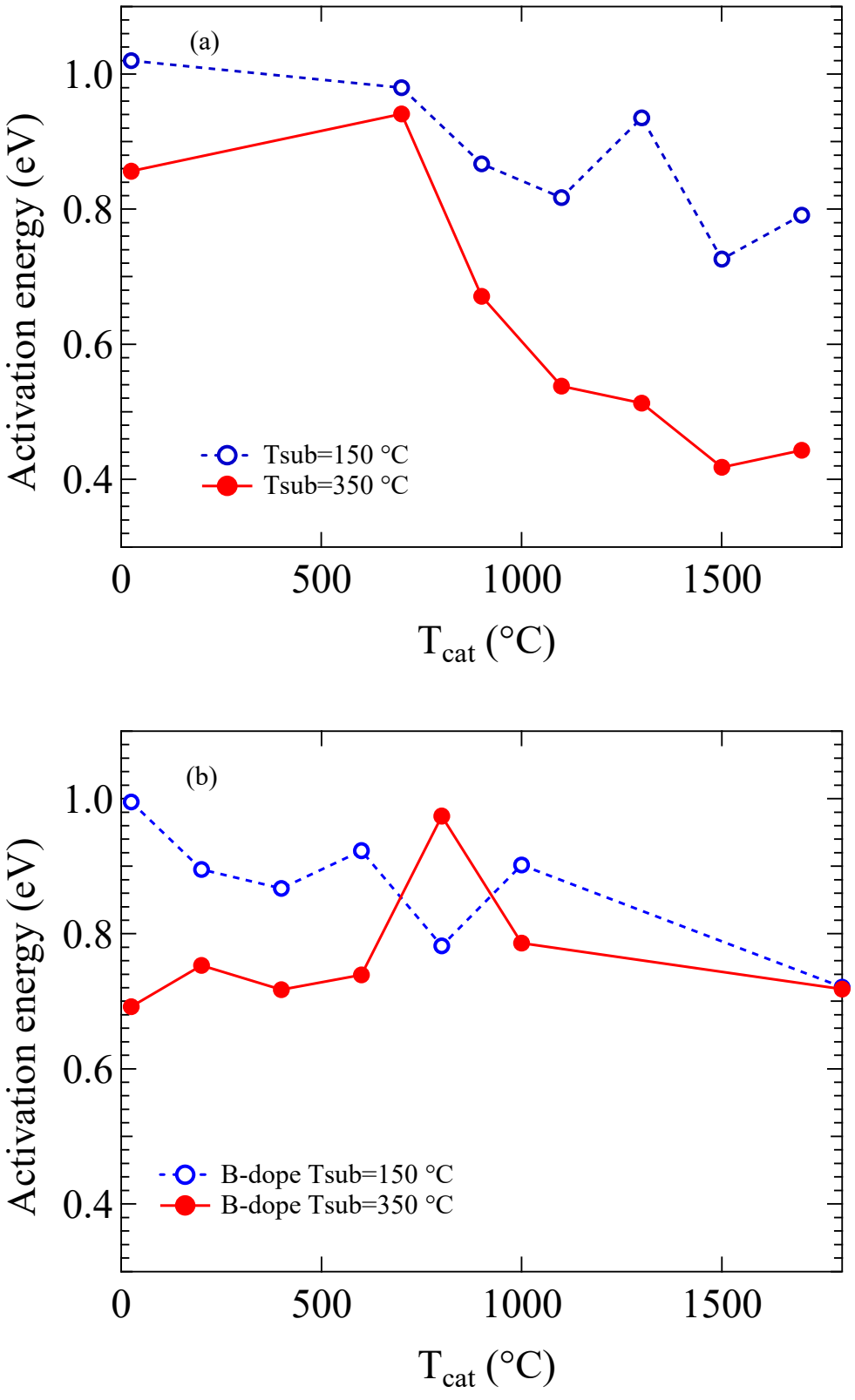

Fig. 3. (Color online)

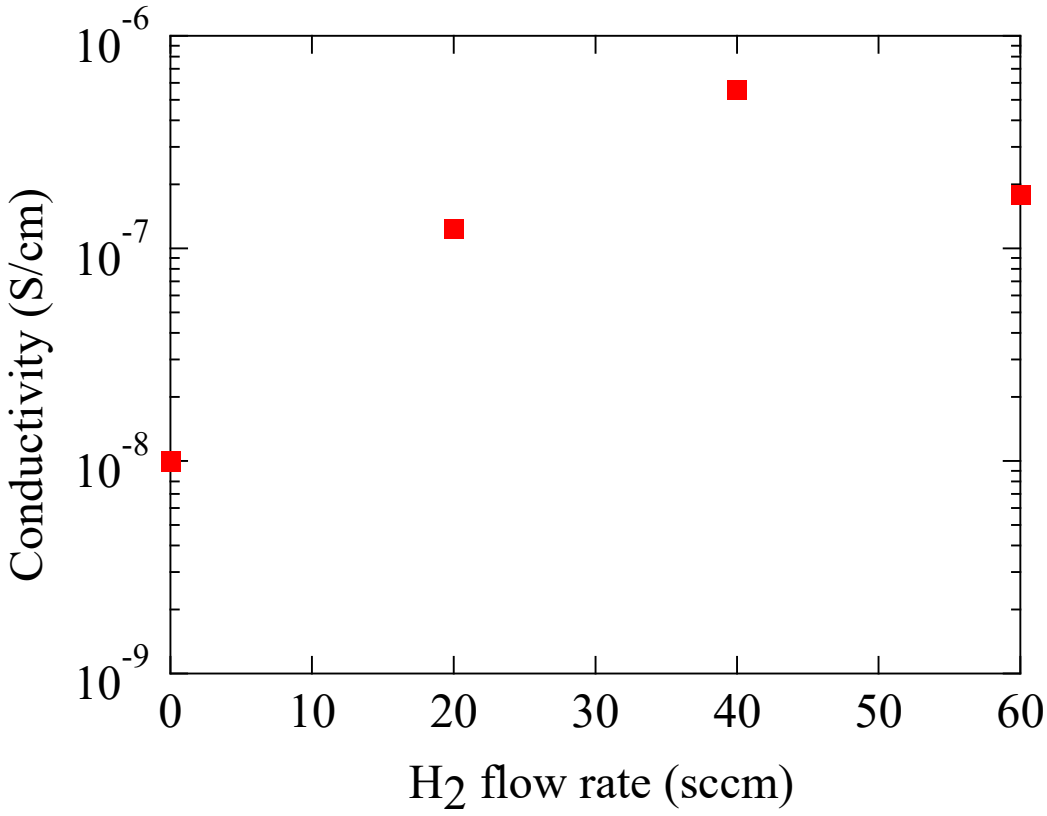

Fig. 4. (Color online)

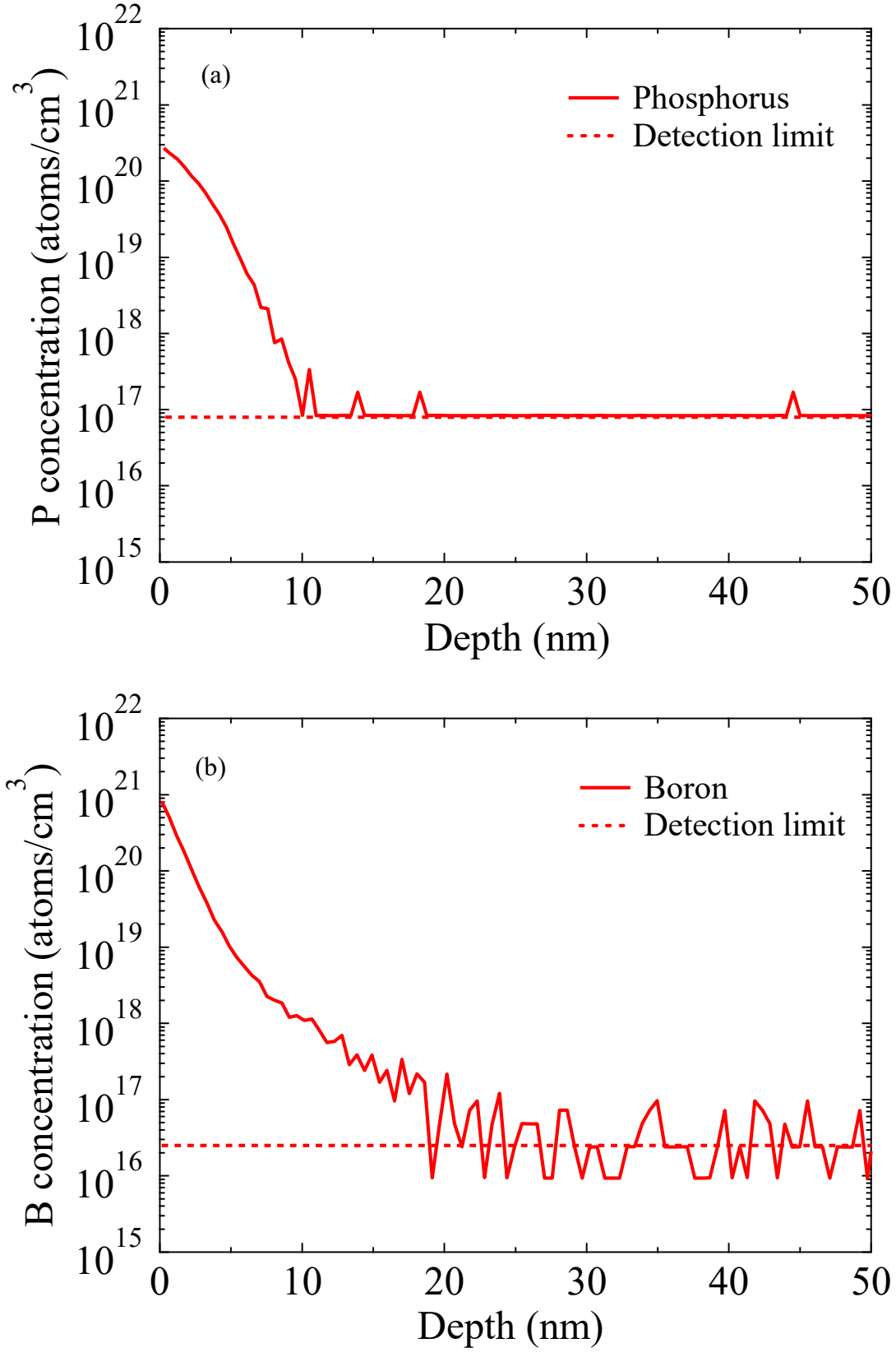

Fig. 5. (Color online)